Discotic liquid crystals of transition metal complexes 48†: Synthesis of novel phthalocyanine-fullerene dyads and effect of a methoxy group on their clearing points

Masahiro Shimizu[a], Lisa Tauchi[a], Takahiro Nakagaki[a], Aya Ishikawa[a], Eiji Itoh[b] and Kazuchika Ohta[a]*

[a]*Smart Material Science and Technology, Interdisciplinary Graduate School of Science and Technology, Shinshu University, 1-15-1 Tokida, Ueda, 386-8567, Japan;* [b]*Department of Electrical and Electronic Engineering, Shinshu University, 4-17-1 Wakasato, Nagano 380-8553, Japan.*

Received date (to be automatically inserted after your manuscript is submitted)
Accepted date (to be automatically inserted after your manuscript is accepted)

ABSTRACT:

In our previous work, we could successfully synthesize the 1:1 phthalocyanine-fullerene (Pc-C_{60}) dyads, (OFbaC_{60})PcCu(OCH_3) **2**, in very high yields (81~96%) by using Prato reaction. In this study, we have prepared novel Pc-C_{60} dyads, (OFbaC_{60})PcM (M = Co (**a**), Ni(**b**), Cu(**c**), metal free(**d**)) **3a-d** without the methoxy group. The target Pc-C_{60} dyads **3a-d** could be successfully synthesized in good yields also by Prato reaction. It is surprising for us that removal of a very small methoxy group from the big (OFbaC_{60})PcCu(OCH_3) molecule (**2**) significantly lowers the cp of (OFbaC_{60})PcCu (**3c**) by about 70^{o}C in comparison with that of **2** having the methoxy group. Very interestingly, each of the novel dyads **3a-d** synthesized here shows perfect homeotropic alignment in the tetragonal columnar phase (Col_{tet}). Moreover, it is noteworthy that **3c** and **3d** show only one $Col_{tet.o}$ mesophase having ordered stacking distance with perfect homeotropic alignment. Such simple phase transition can contribute to maintain stable performance in wide temperature range, when they will be applied to organic thin film solar cells.

KEYWORDS: Discotic liquid crystal, phthalocyanine, fullerene, phthalocyanine-fullerene dyad, homeotropic alignment, organic thin film solar cell

*Correspondence to: Kazuchika Ohta, e-mail: ko52517@ shinshu-u.ac.jp

†Part 47, Tenpei Kamei, Takayuki Kato, Eiji Itoh and Kazuchika Ohta, *J. Porphyrins Phthalocyanines*, 2012, in press.

INTRODUCTION

Liquid crystalline donor-acceptor (D-A) complexes may display superb performance in organic thin film solar cells [1-25]. They can greatly reduce their costs to manufacture the solar cells. Liquid crystalline D-A systems are braodly classified into three groups: smectic liquid crystals [1-4], liquid crystalline copolymers [5-12] and discotic columnar liquid crystals [13-25]. In 2004 Kim *et al.* reported that an organic photovoltaic cell was fabricated by using liquid crystalline N,N'-diheptyl-3,4,9,10-perylenetetracarboxylicdiimide (PTCDI-C7) as the electron acceptor and zinc phthalocyanine (ZnPc) as the electron donor [1]. The two long chain-substituted PTCDI-C7 shows, however, a liquid crystalline phase at very high temperature range (214–403 ^{o}C). In 2007 Hashimoto *et al.* reported that they synthesised a novel liquid crystalline oligothiophene(D)–fullerene(A) dyad to investigate the photovoltaic properties [2]. Moreover, they revealed that the dyad shows a smectic A phase. Liquid crystalline donor–acceptor block copolymers have been also used for photovoltaic applications [5-12]. Morphologies of the vertically oriented mesophase of D–A separated block copolymers are very favorable for organic photovoltaics. Furthermore, the covalent bond between the donor and acceptor blocks is not only desired to improve morphology control, but also to enhance long term stability of the device [8]. However, it seems that the mesophase structure difference between smectic liquid crystals and discotic columnar liquid crystals has been not so much concerned in this field. In comparison with smectic mesophases, discotic columnar mesophases are much easier to realize one-dimensional columnar structure perpendicular to both two electrodes (= homeotropic alignment) [14, 23, 25]. Columnar mesophases in homeotropic alignment are so favourable to obtain higher photoelectric conversion efficiency which can be attributable to larger π-π stacking of the π-conjugated macrocycles [19].

Discotic liquid crystals are well known to spontaneously form one-dimensional columnar structure in their columnar mesophases. Generally, a discotic columnar liquid crystal is composed of a plane and hard central core and several flexible peripheral chains [26]. Especially, triphenylene [27], phthalocyanine (Pc) [28], and porphyrin [28] are often utilized as a central core part. One-dimensional columns can be formed by piling up such disk-like molecules. The column can be a charge carrier path. In order to achieve efficient charge transfer, it is favourable to form perfect homeotropic alignment [14, 19, 23, 25, 29]. On the contrary, it is unfavourable to form both defects and polydomains in the homeotropic alignment [29]. Up to date, there have been some donor-acceptor dyads showing columnar liquid crystalline mesophases [13-25]. For example, Bushby *et al.* reported in 2005 that a triphenylene derivative connected with fullerene showed columnar mesomorphism [13]. This columnar liquid crystalline triphenylene–fullerene dyad partially showed homeotropic alignment, but it has many defective parts. Recently, columnar liquid crystalline phthalocyanine-fullerene dyads [14, 18, 20, 23-25] have been also synthesized.

In 2001, we succeeded in synthesis of phthalocyanine derivatives showing perfect homeotropic alignment in large area at high temperatures [29]. Furthermore, in 2007 we reported the first liquid crystalline phthalocyanine-fullerene dyad, (OMalC_{60})PcCu (**1** in Fig. 1), exhibiting perfect homeotropic alignment in the hexagonal columnar phase (Col_h) at high temperatures [14]. For the synthesis of this phthalocyanine-fullerene dyad **1**, Bingel reaction [30] was adopted to connect phthalocyanine and fullerene. However, it gave polyads connected with two or three phthalocyanines per one fullerene, as the by-products at the same time. Accordingly, the yield of the target 1:1 phthalocyanine-fullerene dyad **1** was very low (20%). Therefore, we changed the synthetic method from Bingel reaction to Prato reaction [31]. By using Prato reaction illustrated in Scheme 1, the 1:1 phthalocyanine-fullerene dyads, (OFbaC_{60})PcM(OCH_3) (**2** in Fig. 1and Scheme 1), could be synthesized in very high yields (81~96%) with negligible amount of undesirable 2:1 phthalocyanine-fullerene by-product [25]. Thus, Prato reaction was more favourable to obtain phthalocyanine-fullerene

dyads than Bingel reaction. The Prato 1:1 phthalocyanine-fullerene dyads **2** also showed perfect homeotropic alignment in the tetragonal columnar phase (Col_{tet}) at high temperatures [25].

In this work, we have synthesized novel phthalocyanine-fullerene dyads, ($OFbaC_{60}$)PcCu (**3** in Fig. 1), by a synthetic route using Prato reaction and another commercially available starting material, as illustrated in Scheme 2. Very interestingly, each of the novel dyads **3** shows perfect homeotropic alignment in the tetragonal columnar phase (Col_{tet}). Moreover, it is surprising for us that removal of a very small methoxy group from the big ($OFbaC_{60}$)PcM(OCH_3) molecule (**2** in Fig. 1) significantly lowers the cp of ($OFbaC_{60}$)PcCu (**3c** in Fig. 1) by about 70^oC in comparison with that of **2** having the methoxy group. We wish to report here the synthesis and very interesting mesomorphic properties and effect of methoxy group on the clearing points of the dyads **3**.

EXPERIMENTS

Synthesis

The synthetic route is shown in Scheme 2. The phthalonitrile derivative, 4,5-bis(3,4-didodecyloxyphenoxy)-1,2-dicyanobenzene (**7**) was prepared by our previously reported method [29]. The phthalocyanine precursors, (OH)PcM (**11**) (**a**: Co, **b**: Ni, **c**: Cu, **d**: metal free), were synthesized from two different phthalonitriles **7** and **10** in a molecular ratio of 3 : 1. The terminal OH group in **11** was esterified with *p*-formyl benzoic acid by Steglich reaction [32] to afford (OFba)PcM (**12**). Finally, ($OFbaC_{60}$)PcM (**3**) was synthesized from **12** with N-methylglycine and fullerene by Prato reaction [31]. These procedures are described below in detail.

4-(12-Hydroxydodecyloxy)phthalonitrile (10)

A mixture of 4-hydroxyphthalonitrile (0.250 g, 1.73 mmol), 12-bromododecanol (0.600 g, 2.25 mmol), K_2CO_3 (0.500 g, 3.62 mmol), and dry DMF (12 ml) was stirred at 160 ^oC under N_2 for 1 h. The reaction mixture was extracted with chloroform and washed with water. The organic layer was dried over Na_2SO_4 and evaporated in *vacuo*. The residue was purified by column chromatography (Silica gel, chloroform : ethyl acetate = 4 : 1, R_f = 0.85). After removal of solvent, 0.479 g of white solid was obtained. Yield = 84.4 %. m.p. = 69.7 ^oC

IR (KBr): ν, cm^{-1} 3536 (-OH), 2918, 2852 (-CH_2-), 2234 (-CN), 1598 (Ar). ^{1}HNMR (4 : 00 MHz; $CDCl_3$; TMS): δ_H, ppm 7.66 (d, 1H, Ar-H), 7.24 (d, 1H, Ar-H), 7.15 (d, 1H, Ar-H), 4 : 01 (t, 2H, -OCH_2), 3.62 (t, 2H, -OCH_2), 2.15 (s, 2H, -CH_2-), 1.53 (s, 16H, -CH_2-), 1.48 (s, 2H, -CH_2-)

2-(12-Hydroxydodecyloxy)-9,10,16,17,23,24-hexakis(3,4-didodecyloxy)phthalocyaninato cobalt ((OH)PcCo: 11a)

A mixture of 4-(12-hydroxydodecyloxy)phthalonitrile (**10**) (70.0 mg, 0.213 mmol), 4,5-bis(3,4-didodecyloxyphenoxy)-1,2-dicyanobenzene (**7**) (0.600 g, 0.572 mmol), $CoCl_2$ (33.0 mg, 0.256 mmol), 1-hexanol (11 ml), and DBU (7 drops) was stirred at 150-160 ^oC under N_2 for 24 h. Ethanol was poured into the reaction mixture to precipitate the target compound. The ethanolic layer was removed by filtration. The residue was extracted with chloroform and washed with water. The organic layer was dried over Na_2SO_4 and evaporated in *vacuo*. The crude product was purified by column chromatography (Silica gel, chloroform, R_f = 0.63) and then recrystallized from ethyl acetate to give 0.155 g of green solid. Yield = 20.5 %.

MS(MALDI-TOF): m/z 3538.11 (calcd. 3536.23)

2-(12-Hydroxydodecyloxy)-9,10,16,17,23,24-hexakis(3,4-didodecyloxy)phthalocyaninato nickel ((OH)PcNi: 11b)

A mixture of 4-(12-hydroxydodecyloxy)phthalonitrile (**10**) (70.0 mg, 0.213 mmol), 4,5-bis(3,4-didodecyloxyphenoxy)-1,2-dicyanobenzene (**7**) (0.600 g, 0.572 mmol), $NiCl_2$ (36.0 g, 0.278 mmol), 1-hexanol (11 ml), DBU (7 drops) was stirred at 150-160 ^oC under N_2 for 17 h. Ethanol was poured into the reaction mixture to precipitate

the target compound. The ethanolic layer was removed by filtration. The residue was extracted with chloroform and washed with water. The organic layer was dried over Na_2SO_4 and evaporated in *vacuo*. The rude product was purified by column chromatography (Silica gel, chloroform, R_f = 0.63) and then recrystallized from ethyl acetate to give 0.162 g of green solid. Yield = 23.7 %.

MS(MALDI-TOF): m/z 3537.22 (calcd. 3536.23)

2-(12-Hydroxydodecyloxy)-9,10,16,17,23,24-hexakis(3,4-didodecyloxy)phthalocyaninato copper ((OH)PcCu:11c)

A mixture of 4-(12-hydroxydodecyloxy)phthalonitrile (**10**) (72.0 mg, 0.219 mmol), 4,5-bis(3,4-didodecyloxyphenoxy)-1,2-dicyanobenzene (**7**) (0.621 g, 0.591 mmol), $CuCl_2$ (38.3 mg,0.285 mmol), 1-hexanol (12 ml), and DBU (7 drops) was stirred at 150-160 ^oC under N_2 for 24 h. Ethanol was poured into the reaction mixture to precipitate the target compound. The ethanolic layer was removed by filtration. The residue was extracted with chloroform and washed with water. The organic layer was dried over Na_2SO_4 and evaporated in *vacuo*. The crude product was purified by column chromatography (Silica gel, chloroform, R_f = 0.55) and then recrystallized from ethyl acetate to give 0.229 g of green solid. Yield = 29.5%.

MS(MALDI-TOF): m/z 354 : 0.54 (calcd. 354 : 0.85)

2-(12-Hydroxydodecyloxy)-9,10,16,17,23,24-hexakis(3,4-didodecyloxy)phthalocyanine ((OH)PcH$_2$:11d)

A mixture of 4-(12-hydroxydodecyloxy)phthalonitrile (**10**) (70.0 mg, 0.213 mmol), 4,5-bis(3,4-didodecyloxyphenoxy)-1,2-dicyanobenzene (**7**) (0.600 g, 0.572 mmol), 1-hexanol (11 ml), DBU (7 drops) was stirred at 150-160 ^oC under N_2 for 24 h. Ethanol was poured into the reaction mixture to precipitate the target compound. The ethanolic layer was removed by filtration. The residue was extracted with chloroform and washed with water. The organic layer was dried over Na_2SO_4 and evaporated in *vacuo*. The crude product was purified by column chromatography (Silica gel, chloroform : n-hexane = 3 : 1, R_f = 0.50) and then recrystallized from ethyl acetate to give 0.188 g of green solid. Yield = 27.9 %.

MS(MALDI-TOF): m/z 3482.63 (calcd. 3479.32)

Cobalt benzoic derivative ((OFba)PcCo: 12a)

A mixture of (OH)PcCo (**11a**) (0.120 g, 0.0339 mmol), *p*-formyl benzoic acid (11.5 mg, 0.0763 mmol), *N,N'*-dicyclohexylcarbodiimide (70.0 mg, 0.339 mmol), *N,N*-dimethyl-4-aminopyridine (12.4 mg, 0.102 mmol), and dry CH_2Cl_2 (20 ml) was stirred at r.t. under N_2 for 30 h. The reaction mixture was extracted with chloroform and washed with water. The organic layer was dried over Na_2SO_4 and evaporated in *vacuo*. The residue was purified by column chromatography (Silica gel, chloroform, R_f = 0.90) and then recrystallized from ethyl acetate to give 0.108 g of green solid. Yield = 87.3 %.

MS(MALDI-TOF): m/z 3671.58 (calcd. 3667.34)

Nickel benzoic derivative ((OFba)PcNi:12b)

A mixture of (OH)PcNi (**11b**) (0.120 g, 0.0339 mmol), *p*-formyl benzoic acid (11.2 mg, 0.0747 mmol), *N,N'*-dicyclohexylcarbodiimide (70.0 mg, 0.339 mmol), *N,N*-dimethyl-4-aminopyridine (12.4 mg, 0.102 mmol), and dry CH_2Cl_2 (20 ml) was stirred at r.t. under N_2 for 24 h. The reaction mixture was extracted with chloroform and washed with water. The organic layer was dried over Na_2SO_4 and evaporated in *vacuo*. The residue was purified by column chromatography (Silica gel, chloroform, R_f = 0.89) and then recrystallized from ethyl acetate to give 0.122 g of green solid. Yield = 98.7 %.

MS(MALDI-TOF): m/z 3670.47 (calcd. 3667.34)

Copper benzoic derivative ((OFba)PcCu:12c)

A mixture of (OH)PcCu (**11c**) (0.150 g, 0.0424 mmol), *p*-formyl benzoic acid (9.53 mg, 0.0635 mmol), *N,N'*-dicyclohexylcarbodiimide (13.1 mg, 0.0635mmol), *N,N*-dimethyl-4-aminopyridine (31.0 mg, 0.254 mmol), and dry

CH_2Cl_2 (15 ml) was stirred at r.t. under N_2 for 24 h. The reaction mixture was extracted with chloroform and washed with water. The organic layer was dried over Na_2SO_4 and evaporated in *vacuo*. The residue was purified by column chromatography (Silica gel, chloroform, R_f = 0.90) and then recrystallized from ethyl acetate to 0.102 g of give green solid. Yield = 65.0 %.

MS(MALDI-TOF): m/z 3676.71 (calcd. 3671.96)

Metal free benzoic derivative ((OFba)PcH$_2$:12d)

A mixture of (OH)PcH_2 (**11d**) (0.120 g, 0.0349 mmol), *p*-formyl benzoic acid (7.76 mg, 0.0517 mmol), *N,N'*-dicyclohexylcarbodiimide (10.7 mg, 0.0517 mmol), *N,N*-dimethyl-4-aminopyridine (25.3 mg, 0.207 mmol), and dry CH_2Cl_2 (11 ml) was stirred at r.t. under N_2 for 24 h. The reaction mixture was extracted with chloroform and washed with water. The organic layer was dried over Na_2SO_4 and evaporated in *vacuo*. The residue was purified by column chromatography (Silica gel, chloroform : n-hexane = 10 : 1, R_f = 0.93) and then recrystallized from ethyl acetate to give 0.0844 g of green solid.. Yield = 66.5 %.

MS(MALDI-TOF): m/z 3614.27 (calcd. 3610.43)

Cobalt fullerene derivative ((OFbaC$_{60}$)PcCo: 3a)

A mixture of (OFba)PcCo (**12a**) (50.0 mg, 0.0136 mmol), C_{60} fullerene (19.6 mg, 0.0272 mmol), *N*-methylglycine (2.91 mg 0.0326 mmol), and dry toluene (80 ml) was stirred at 120 ^oC under N_2 for 24 h. The reaction mixture was extracted with chloroform and washed with water. The organic layer was dried over Na_2SO_4 and evaporated in *vacuo*. Unreacted fullerene was removed by chromatography (Silica gel, toluene, R_f = 1.0), and the residue in silica gel was flushed out with THF. The crude product was recrystallized from ethyl acetate at r.t. and THF at -20 ^oC, respectively. After removal of solvent, 47.9 mg of green solid was obtained. Yield = 79.8 %.

MS(MALDI-TOF): m/z 4416.57 (calcd. 4415.07)

Nickel fullerene derivative ((OFbaC$_{60}$)PcNi: 3b)

A mixture of (OFba)PcNi (**12b**) (60.0 mg, 0.0164 mmol), C_{60} fullerene (23.6 mg, 0.0327 mmol), *N*-methylglycine (2.92 mg 0.0328 mmol), and dry toluene (90 ml) was stirred at 120 ^oC under N_2 for 14 h. The reaction mixture was extracted with chloroform and washed with water. The organic layer was dried over Na_2SO_4 and evaporated in *vacuo*. Unreacted fullerene was removed by chromatography (Silica gel, toluene, R_f = 1.0), and the residue in silica gel was flushed out with THF. The crude product was recrystallized from ethyl acetate at r.t. and THF at -20 ^oC, respectively. After removal of solvent, 70.1 mg of green solid was obtained. Yield = 96.8 %.

MS(MALDI-TOF): m/z 4424.4 (calcd. 4415.07)

Copper fullerene derivative ((OFbaC$_{60}$)PcCu: 3c)

A mixture of (OFba)PcCu (**12c**) (60.0 mg, 0.0163 mmol), C_{60} fullerene (23.4 mg, 0.0325 mmol), *N*-methylglycine (3.47 mg 0.0389 mmol), and dry toluene (60 ml) was stirred at 120 ^oC under N_2 for 14 h. The reaction mixture was extracted with chloroform and washed with water. The organic layer was dried over Na_2SO_4 and evaporated in *vacuo*. Unreacted fullerene was removed by chromatography (Silica gel, toluene, R_f = 1.0), and the residue in silica gel was flushed out with THF. The crude product was recrystallized from ethyl acetate at r.t. and THF at -20 ^oC, respectively. After removal of solvent, 61.3 mg of green solid was obtained. Yield = 85.1 %.

MS(MALDI-TOF): m/z 4424.18 (calcd. 4419.69)

Metal free fullerene derivative ((OFbaC$_{60}$)PcH$_2$: 3d)

A mixture of (OFba)PcH_2 (**12d**) (47.0 mg, 0.0130 mmol), C_{60} fullerene (18.7 mg, 0.0259 mmol), *N*-methylglycine (2.77 mg 0.0311 mmol), and dry toluene (65 ml) was stirred at 120 ^oC under N_2 for 14 h. The reaction mixture was extracted with chloroform and washed with water. The organic layer was dried over Na_2SO_4 and evaporated in *vacuo*. Unreacted fullerene was removed by chromatography (Silica gel, toluene, R_f = 1.0), and the residue in silica gel was

flushed out with THF. The crude product was recrystallized from ethyl acetate at r.t. and THF at -20 ^{o}C, respectively. After removal of solvent, 43.0 mg of green solid was obtained. Yield = 75.8 %.

MS(MALDI-TOF): m/z 4366.84 (calcd. 4358.16)

Measurements

The ^{1}H-NMR measurements were carried out by using ^{1}H-NMR (BRUKER Ultrashield 400 M Hz). The elemental analyses were performed by using a Yanaco CHN CORDER MT-3. The MALDI-TOF mass spectral measurements were carried out by using a PerSeptive Biosystems Voyager DE-Pro spectrometer (matrix: dithranol). Infrared absorption spectra were recorded by using a Nicolet NEXUS670 FT-IR. Electronic absorption (UV-vis) spectra were recorded by using a HITACHI U-4100 spectrophotometer. Phase transition behaviour of the present compounds was observed with polarizing optical microscope (Nikon ECLIPSE E600 POL) equipped with a Mettler FP82HT hot stage and a Mettler FP-90 Central Processor, and differential scanning calorimeter (Perkin-Elmer Diamond DSC.) The mesophases were identified by using a wide angle X-ray diffractometer (Rigaku Rad) equipped with Cu-Kα radiation and a handmade hot stage equipped with a temperature controller [33].

RESULTS AND DISCUSSION

Synthesis of the novel Pc compounds: 11a-d, 12a-d, and 3a-d

Table 1 summarizes MALDI-TOF mass spectra data, elemental analysis results, and yields of **11a-d**, **12a-d**, and **3a-d**. The 3 : 1 precursors, (OH)PcM (**11**), could be prepared in 20-30% of yields. These low yields are resulted from the inevitable by-product of the 4 : 0 phthalocyanine composed of only 4,5-bis(3,4-didodecyloxyphenoxy)-1,2-dicyanobenzene units. On the other hand, the precursors, (OFba)PcM (**12**), could be prepared in good yields by Steglich esterification [32]. The corresponding dyads, (OFbaC_{60})PcM (**3**), were synthesized by Prato reaction [31]. All the products gave satisfactory molecular weights by MALDI-TOF mass spectra. The elemental analysis data of the precursors **11** and **12** agreed with the theoretical values. However, the dyads **3a-d** did not completely burnt out at the measurement temperature (850^{o}C). Therefore, these elemental analysis data are not listed up in Table 1. Electronic absorption (UV-vis) spectra were recorded in order to confirm the existence of the phthalocyanine and fullerene parts. In Table 2 are listed electronic spectral data of all the compounds, **11**, **12** and **3**. The UV-vis spectra are illustrated in Fig. 2. As can be seen from these table and figure, each of the compounds **11**, **12** and **3**, shows Q-band (600-700nm) and Soret band (300-400nm) characteristic to the phthalocyanine macrocycle. As can be seen from Fig. 2d, each of the Pc compounds **3d**, **11d** and **12d** gave split Q-band characteristic to a metal free phthalocyanine. Each of the dyads **3a-d** gave an additional absorption peak at ca.250nm attributed to fullerene moiety, whereas the other phthalocyanine precursors, **11a-d** and **12a-d**, did not give this peak. This fact clearly supports that fullerene is connected with phthalocyanine in the dyads **3a-d**. Thus, we confirmed that all the target Pc-fullerene dyads **3** could be successfully synthesized.

Although we tried to measure ^{1}H-NMR spectra of the diamagnetic Pc derivatives, **11b,d**, **12b,d** and **3b,d**, all our attempts were in vain. As is well-known, phthalocyanine discotic liquid crystals tend to aggregate even in a very dilute chloroform solution like as 10^{-6} mol/L. We could not measure ^{1}H-NMR spectra for such a dilute solution. So, we need to increase the concentration to ca. 10^{-3} mol/L for the NMR measurements. However, very strong aggregation took place in such a concentrated solution, and it always gave the very broad meaningless NMR spectra. Accordingly, we used the other solvents, d6-DMSO and/or d8-THF, for the Pc-C_{60} dyads, **3b,d,** but the dyads were totally insoluble in DMSO and less soluble in THF than chloroform. Even for the saturated solution in hot d8-THF, it gave a very broad meaningless

^{1}H-NMR spectrum due to the strong aggregation. Thus, all our trials were in vain for the NMR measurements. However, as mentioned above we confirmed from MALDI-TOF mass spectra and the UV-vis spectra that all the target Pc-fullerene dyads **3** could be successfully synthesized.

Unusual Phase transition behaviour of 11 and 12

The phase transition behaviour of the PcM precursors (**11** and **12**) and the PcM-C_{60} dyads (**3**) is summarized in Table 3. Their X-ray data of **11**, **12** and **3** are listed in Table 4. The phase transition behaviour was revealed by polarization microscopy (POM), differential scanning calorimetry (DSC), temperature-dependent X-ray diffraction measurements and temperature-dependent electronic spectrometry.

As can be seen from Table 3, each of the (OH)PcM derivatives (**11a-d**) shows very interesting phase transition sequence, *e.g.*, K(R) → Col_{tet}(R) → Col_h(F) → Col_{tet}(F) → I.L.for (OH)PcNi (**11b**) on heating stage. (R) and (F) mean roof-top-shaped dimer stacking and face-to-face stacking, respectively. On cooling from I.L., it gave Cub(Pn3m). On further cooling the Cub phase relaxed into Col_{tet}(F) and then it transformed into Col_h(F). The Col_h(F) mesophase was supercooled till r.t. Thus, the (OH)PcNi (**11b**) derivative gave a very peculiar phase transition like as Col_{tet}(R) → Col_h(F) → Col_{tet}(F). As can be seen from Table 3, the (OFba)PcNi (**12b**) derivative also showed unusual phase transitions like as K(R) → Col_{tet}(R) → Col_{tet}(F) → I.L. on heating stage, and I.L. → Cub(Pn3m) → M_x → Col_h(R) → Col_{tet}(R) → K(R) on cooling stage. These unusual phase transition sequences of **11** and **12** are resulted from formation, deformation, and reformation of roof-top-shaped dimers.

Formation, deformation and reformation of the roof-top-shaped dimers of 11 and 12

UV-vis spectra of the thin film certified the roof-top-shaped dimer formation, which is based on Kasha's rule [34] for the excited energy levels as illustrated in Fig. 3. As can be seen from Fig. 3d, when roof-top-shaped dimers are formed, the excited energy level is split into two levels. Hence, the Q-band of phthalocyanine should be split into two peaks only in the roof-top-shaped dimer. Representative UV-vis spectra of the thin films of **11b**, **12b**, and **3b** are shown in Fig. 4. The Col_{tet}(R) mesophase of **11b** at 80^{o}C gave a shoulder at ca. 750nm. The peak at ca.680nm and the shoulder at ca. 750nm correspond to two split Q-bands. However, the shoulder at ca. 750nm disappeared with heating and did not appear again on cooling. On the other hand, the Col_{tet}(R) mesophase of **12b** at 80^{o}Cgave a much clearer shoulder at ca. 750nm. Although the shoulder at ca. 750nm disappeared on further heating, it appeared again for the Col_h(R) mesophase on cooling stage.

These spectral changes agree with the stacking distances in the XRD data listed in Table 4. As can be seen from this table, the Col_{tet}(R) mesophase of **11b** at 80^{o}C, for example, gave a sharp peak at 4.87Å (h_1) and a broad peak at *ca.* 9.4Å (h_2: approximately two times of 4.87Å). Taking into account these two stacking distances at 4.87Å and two times of the stacking distance at *ca.* 9.2Å, it is consistent with formation of the roof-top-shaped dimers in the columns. When it was further heated up into the Col_h(F) mesophase at 105^{o}C, the peak at 4.87Å disappeared and a broad peak appeared at *ca.* 3.5Å instead, as listed in this table. Stacking distance of *ca.* 3.5Å is a typical stacking distance of phthalocyanine disks stacked face-to-face. Therefore, the roof-top-shaped dimers in the Col_{tet}(R) mesophase changed into face-to-face stacking in the Col_h(F) mesophase at the phase transition from Col_{tet}(R) to Col_h(F) at 92.0^{o}C. As can be seen from Table 3, the Col_h(F) mesophase changed into another tetragonal mesophase, Col_{tet}(F), at 110.3^{o}C, which cleared into isotropic liquid (I.L.) at 172.3^{o}C. It is very interesting that a Cub mesophase, Cub(Pn3m), appeared only on cooling from I.L. and it also gave a short stacking distance at *ca.* 3.5 Å (h). On further cooling below 110.3, the Col_h(F) mesophase appeared again via Col_{tet}(F). The Col_h(F) mesophase gave again the broad peak at *ca.* 3.5Å in the X-ray diffraction pattern. On further cooling, the Col_h(F) mesophase was suppercooled until room temperature and the stacking distance at *ca.* 3.5Åwas maintained.

For another example, the Col_{tet}(R) mesophase of **12b** at 90°C also gave two stacking distances at 4.85 Å (h_1) and ca. 9.3 Å (h_2: approximately two times of 4.85Å), whereas the higher temperature mesophase Col_{tet}(F) at 160°C gave a short stacking distance at *ca.* 3.5 Å (h), as can be seen from Table 4. Very interestingly, the Cub(Pn3m) mesophase of **12b** also appeared only on cooling from I.L. and it gave a short tacking distance at *ca.* 3.5 Å (h). On further cooling, Col_h(R) mesophase appeared and gave two stacking distances at 4.85 Å (h_1) and ca. 9.5 Å (h_2). These formation, deformation and reformation of the roof-top-shaped dimer are compatible with the UV-vis spectral changes of the thin film of **12b** mentioned above.

These unique phase structural changes of the representative (OFba)PcNi (**12b**) derivative are illustrated in Fig. 5, together with the phase transition sequence.

Phase transition behaviour of 3

As can be seen from Table 3, each of the Pc-C_{60} dyads, (OFbaC_{60})PcM (**3a-d**), shows only tetragonal columnar (Col_{tet}) mesophase(s). As can be seen from Table 4, the $Col_{tet.o}$ mesophases of **3b-d** gave a longer stacking distance at ca.4.85 Å, which was observed as a roof-top-shaped dimer stacking distance for the Pc precursors, **11a-d** and **12a-d**. However, as can be seen from Fig. 4, the representative Pc-C_{60} dyad **3b** did not show split Q bands, and the UV-vis spectra did not change at all for the heating and cooling cycle. Therefore, it can be concluded that **3b** does not form the roof-top-shaped dimers, and that the face to-face stacking shape maintains at all temperatures.

This phenomenon may be attributed to the size of substituent group. The precursors **11** and **12** having a relatively small terminal substituent group of hydroxyl or *p*-formyl benzoate hardly move in more frozen alkyl chains at lower temperatures. Accordingly, the phthalocyanine core parts having the relatively small terminal substituent groups may tend to form roof-top-shaped dimers in the lower temperature mesophases of Col_{tet}(R) and Col_h(R). On the other hand, these relatively small terminal substituent group can easily move in more melted alkyl chains in Col_{tet}(F) mesophase at higher temperatures. As a result, phthalocyanine core parts easily stack face-to-face in the higher temperature mesophases of Col_{tet}(F) and Cub(Pn3m). Therefore, two longer stacking distances of 4.85Å and *ca.* 9.5Å appear at lower temperature mesophases, whereas a short stacking distance at ca. 3.5Å appears at higher temperature mesophases. The Pc disks of Pc-C_{60} dyad **3b** having very bulky terminal substituent group of fullerene may not tilt to form roof-top-shaped dimer due to the bulkiness of fullerene at all the temperatures. Therefore, the dyad **3b** may keep their stacking shape face-to-face at 4.85Å.

Compared with the clearing points (cps) in Table 3 for all the present derivatives **11a-d**, **12a-d**, and **3a-d** having a different terminal group, the cps of **12a-d** having benzoic acid group are lower by about 6°C on the average than those of **11a-d** having OH group. The cps of **3a-d** having fullerene group is lower by about 67°C on the average than those of **12a-d** having benzoic acid group. Therefore, the bulkier the terminal substituted group becomes in an order of OH < benzoic acid < fullerene, the more Col_{tet} mesophase only tends to appear.

Additionally, the dyads **3a-d** only showed gradual decomposition over their cps. It may be resulted from charge transfer from Pc moiety to fullerene. Further studies are needed to clarify the origin of this decomposition.

Effect of an additional methoxy group directly substituted to Pc core on clearing points

In our previous work [2425], we successfully synthesized PcCu derivatives, (OH)PcCu(OCH_3) (**8**), (OFba)PcCu(OCH_3) (**9**) and (OFbaC_{60})PcCu(OCH_3) (**2**), which have an additional methoxy group directly substituted to Pc core, as shown in Scheme 1. In contrast to these previous derivatives, the present PcCu derivatives, (OH)PcM (**11c**), (OFba)PcM (**12c**) and (OFbaC_{60})PcM (**3c**), have no additional methoxy group, as can be seen from Scheme 2. Therefore, it is very interesting for us to investigate the effect of an additional methoxy group on their phase transition behaviour. Table 5 lists the phase transition behaviour of the representative derivatives in both series for comparison.

Comparing these clearing points, the present PcCu compounds (**11c**, **12c** and **3c**) give lower clearing points than the previous methoxy-group-substituted PcCu derivatives (**8**, **9** and **2**): the cp of **11c** is lower about 15°C than that of **8**; the cp of **12c** is about 10°C than that of **9**; and the cp of **3c** is about 70°C than that of **2**. It is surprising for us that removal of such a small methoxy group from the big (OFbaC$_{60}$)PcM(OCH$_3$) (**2**) molecule significantly lowers the cp of (OFbaC$_{60}$)PcCu (**3c**) by about 70°C in comparison with that of **2** having the methoxy group. Although the reason of the cp lowering is not clear at the present stage, we tentatively speculate it as follows. The present PcCu compounds (**11c**, **12c** and **3c**) have larger open space around Pc macrocycle than the previous methoxy-group-substituted PcCu derivatives (**8**, **9** and **2**). Therefore, the bulky terminal fullerene group of the neighbouring molecule may reach more closely to the Pc macrocycle and perturb the stacking of Pc disks to destroy the columnar structure effectively at much lower temperatures; it may cause the cp lowering the present PcCu compounds (**11c**, **12c** and **3c**).

As can be seen from Table 5, each of the PcCu derivatives in both series shows homeotropic alignment in the highest temperature Col$_{tet}$ mesophase.

Homeotropic alignment

As can be seen from Table 3, each of the present novel Pc compounds, **11** and **12**, shows homeotropic alignment in the highest temperature Col$_{tet}$ mesophase. On the other hand, each of the Pc-C$_{60}$ dyads **3** shows homeotropic alignment in all the Col$_{tet}$ mesophases. When perfect homeotropic alignment can be achieved, it will give complete darkness between cross polarizers. As can be seen from the photomicrographs in Fig. 6, the (OFbaC$_{60}$)PcM (M = Co, Ni, Cu, H$_2$) dyads, **3a-d,** in the Col$_{tet}$ mesophases exhibited complete darkness characteristic to perfect homeotropic alignment. It is noteworthy that **3c** and **3d** show only one Col$_{tet.o}$ mesophase having ordered stacking distance with perfect homeotropic alignment. Such simple phase transition can contribute to maintain stable performance in wide temperature range, when they will be applied to organic thin film solar cells.

CONCLUSIONS

In this study, we have successfully prepared novel PcM compounds, **11a-d** and **12a-d**, and Pc-C$_{60}$ dyads **3a-d** (**M=** Co (**a**), Ni(**b**), Cu(**c**), metal free(**d**)). The Pc-C$_{60}$ dyads **3a-d** could be obtained in good yields by Prato reaction. We established their unique mesomorphism using temperature-dependent X-ray diffraction measurements and temperature-dependent electronic spectroscopy. It is surprising for us that a small methoxy group largely affects the cps of these big molecules, especially cps of Pc-C$_{60}$ dyads. The cp of **3c** having no methoxy group is lower about 70°C than that of **2** having the methoxy group. Each of the present novel Pc compounds, **11** and **12**, shows homeotropic alignment in the highest temperature Col$_{tet}$ mesophase. On the other hand, each of the Pc-C$_{60}$ dyads **3** shows homeotropic alignment in all the Col$_{tet}$ mesophases. Very interestingly, the Pc-C$_{60}$ dyads **3c** and **3d** showed simple phase transition with perfect homeotropic alignment in Col$_{tet.o}$ mesophase having ordered stacking distance. These properties are very suitable for organic solar cell fabrication.

Acknowledgement

This work is partially supported by Grant-in-Aid for science research (Grant No. 2236012311) from the Ministry of Education, Culture, Sports, Science and Technology, Japan.

REFERENCES

1. Kim JY, Bard AJ. *Chem. Phys. Lett.* 2004; **383**: 11–15.

2. Nishizawa T, Tajima K, Hashimoto K. *J. Mater. Chem.* 2007; **17**: 2440–2445.
3. Roland T, Ramirez GH, Léonard J, Méry S, Haacke S. *J. Phys.: Conference Series* 2011; **276**: 012006(1-6).
4. Lincker F, Heinrich B, Bettignies R, Rannou P, Pecaut J, Grevin B, Pron A, Donnio B, Demadrille R. *J. Mater. Chem.* 2011; **21**: 5238-5247.
5. Barrau S, Heiser T, Richard F, Brochon C, Ngov C, van de Wetering K, Hadziioannou G, Anokhin DV, Ivanov DA. *Macromolecules.* 2008; **41**: 2701-2710.
6. Kim DH, Lee BL, Moon H, Kang HM, Jeong EJ, Park JI, Han KM, Lee S, Yoo BW, Koo BW, Kim JY, Lee YH, Cho K, Becerril HA, Bao Z. *J. Am. Chem. Soc.* 2009; **131**: 6124-6132.
7. Liang TC, Chiang IH, Yang PJ, Kekuda D, Chu CW, Lin HC. *J. Poly. Sci.: Part A Poly. Chem.* 2009; **47**: 5998-6013
8. Sommer M, Huettner S, Thelakkat M. *J. Mater. Chem.* 2010; **20**; 10788–10797.
9. Yao K, Chen Y, Chen L, Li F, Li X, Ren X, Wang H, Liu T. *Macromolecules.* 2011; **44**: 2698–2706.
10. Yasuda T, Yonezawa K, Ito M, Kamioka H, Han L, Moritomo Y. *J. Photopolym. Sci. Technol.* 2012; **25**: 271-276.
11. Han Y, Chen L, Chen Y. *J. Poly. Sci. Poly. Chem*. 2012; published online: DOI: 10.1002/pola.26394.
12. Li F, Chen W, Chen Y. *J. Mater. Chem*. 2012; **22**: 6259-6266.
13. Bushby JR, Hamley IW, Liu Q, Lozman OR, Lydon EJ. *J Mater Chem*. 2005; **15**: 4429-4434.
14. Uchida S, Kude Y, Nishikitani Y, Ota (= Ohta) K. *Jpn. Kokai Tokkyo Koho*. JP 2008214227(A)-2008-09-18 (Priority number: JP2007060604; Submission Date: 2007-03-09)
15. Zhou X, Kang SW, Kumar S, Kulkarni RR, Cheng SZD, Li Q. *Chem. Mater*, 2011; **20**: 3551-3553.
16. de la Escosura A, Martınez-Dıaz MV, Barbera J, Torres T. *J. Org. Chem.*, 2008; **73**; 1475-1480.
17. Tashiro K, Aida T. *J Amer. Chem. Soc*. 2008; **130** ; 13812–13813.
18. Geerts YH, Debever O, Amato C, Sergeyev S. *Beilstein J. Org. Chem.*, *Beilstein J. Org. Chem.* 2009; **5**, 1-9.
19. Thiebaut O, Bock H, and Grelet E. *J. Am. Chem. Soc.* 2010; **132**: 6886–6887.
20. Hayashi H, Nihashi W, Umeyama T, Matano Y, Seki S, Shimizu Y, Imahori H. *J. Am. Chem. Soc.* 2011; **133** : 10736–10739.
21. Bagui M, Dutta T, Chakraborty S, Melinger JS, Zhong H, Keightley A, Peng Z. *J. Phys. Chem. A* 2011; **115**: 1579–1592.
22. Haverkate LA, Zbiri M, Johnson MR, Deme B, de Groot HJM, Lefeber F, Kotlewski A, Picken SJ, Mulder FM, Kearley GJ. *J. Phys. Chem. B* 2012; **116**: 13098-13105.
23. Ota (= Ohta) K. *Jpn. Kokai Tokkyo Koho*, JP2011132180(A)-2011-07-07 (Priority number: JP20090293501; Submission Date: 2009-12-24).
24. Ince M, Martinez-Diaz MV, Barbera, J, Torres, T. *J. Mater. Chem.* 2011; **21**: 1531-1536.
25. Kamei T, Kato T, Itoh E, Ohta K. *J. Porphyrins Phthalocyanines* 2012; in press.
26. Demus D, Goodby J, Gray GW, Spiess HW, Vill V. *Handbook of Liquid Crystals*, vol. 2B. Wiley-VCH, New York, 1998; 693-798.
27. Kumar S. *Chemistry of Discotic Liquid Crystals: From Monomers to Polymers*, CRC Press: 2010.
28. Ohta K, Nguyen-Tran H.-D, Tauchi L, Kanai Y, Megumi T and Takagi Y. *Chapter 53: Liquid Crystals of Phthalocyanines, Porphyrins and Related Compounds* in *Handbook of Porphyrin Science*, Vol. 12. World Scientific Publishing: Singapore, 2011; pp 1–120.
29. Hatsusaka K, Ohta K, Yamamoto I and Shirai H. *J. Mater. Chem.* 2001; **11**: 423–433.
30. Bingel C. Chem. Ber. 1993; **126**: 1957-1959.
31. Maggini M, Scorrano G, Prato M. *J. Am. Chem. Soc*. 1993; **115**: 9798-9799.
32. Neises B, Steglish W. *Angew. Chem. Int. Ed.* 1978; **17**: 522-524.

33. Hasebe H. Master Thesis, Sinshu University (1991); Ema H. Master Thesis, Sinshu University (1988).
34. Kasha M, Rawls HR, El-Bayoumi MA. *Pure. Appl. Chem.* 1965; **11**: 371.

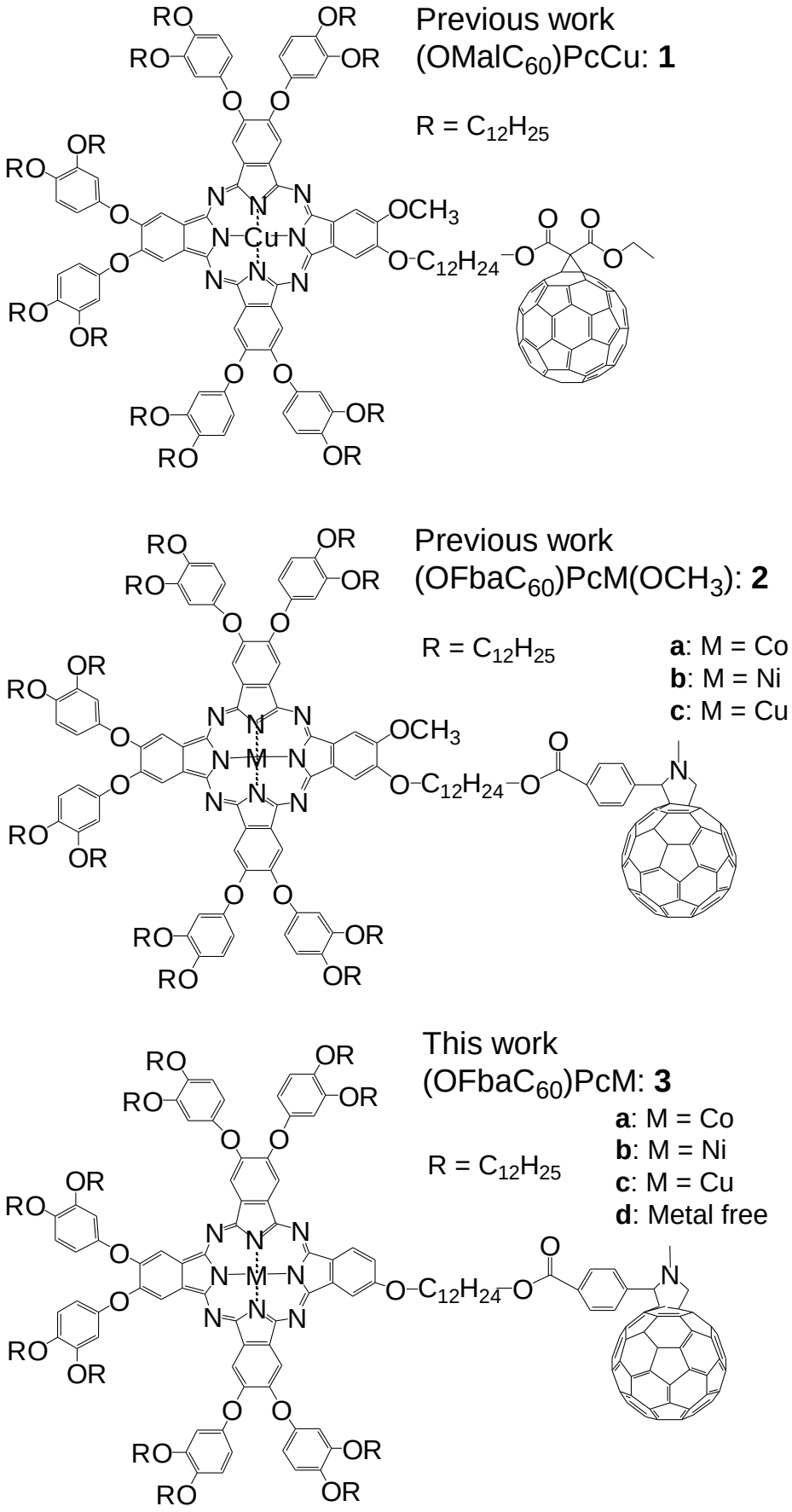

Fig. 1 Molecular formulae of the previous Pc-C_{60} dyads (**1**, **2**) and the present Pc-C_{60} dyad(**3**)**.**

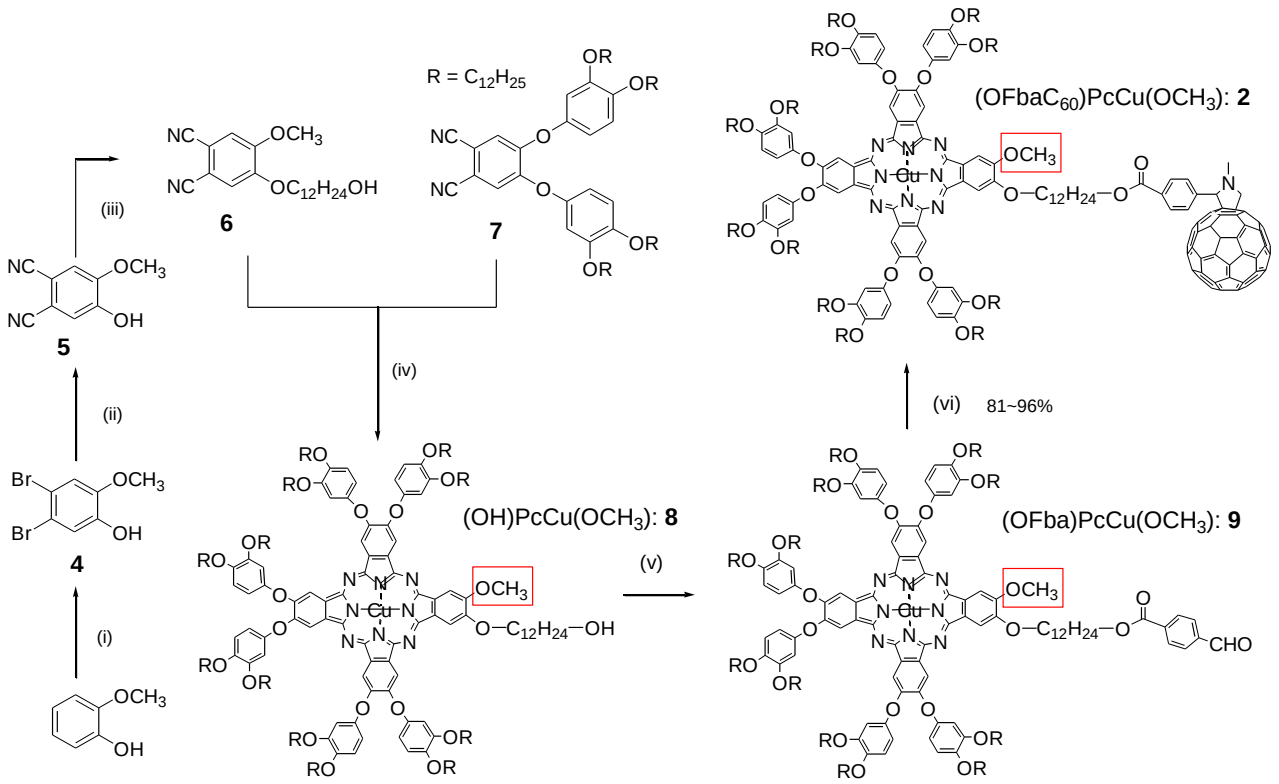

Scheme 1 Synthetic route for the previous Pc-C_{60} dyad, (OFbaC$_{60}$)PcCu(OCH$_3$): **2**, by using Prato Reaction. (i) Br_2 / $(C_2H_5)_2O{\bullet}BF_3$, $CHCl_3$ / CH_2Cl_2; (ii) CuCN, DMF; (iii) $BrC_{12}H_{24}OH$, K_2CO_3 / DMF; (iv) DBU/ $CuCl_2$, *n*-hexanol; (v) *p*-Formylbenzoic acid, DMAP / DCC, CH_2Cl_2; (vi) N-Metylglycine, C_{60} / toluene. DMAP = 4-Dimethylaminopridine. DCC = N,N-Dicyclohexylcarbodiimide.

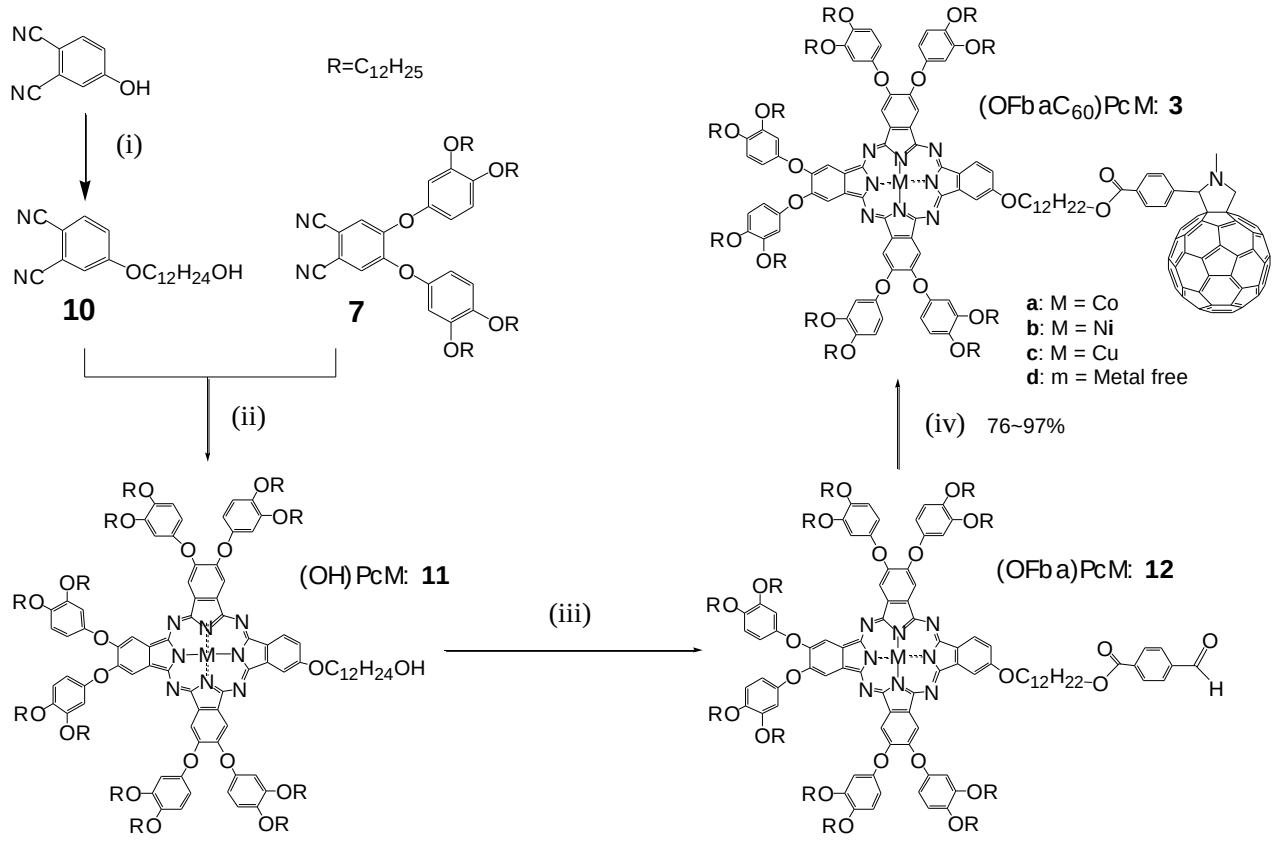

Scheme 2 Synthetic route for novel Pc-C_{60} dyads, (OFbaC$_{60}$)PcM: **3a-d**, by using Prato Reaction. (i) $BrC_{12}H_{24}OH$, K_2CO_3 / DMF; (ii) MCl_2, DBU, *n*-hexanol ; (iii) *p*-Formylbenzoic acid, DMAP / DCC, CH_2Cl_2; (iv) N-Metylglycine, C_{60} / toluene. DMF = *N.N'*-dimethylformamide, DBU = 1,8-diazabicyclo[5,4,0]-7-undecene, DMAA = *N,N*-dimethylacetamide, DCC = *N,N'*-dicyclohexylcarbodiimide, and DMAP = *N,N*-dimethyl-4-aminopyridine.

Table 1 MALDI-TOF mass spectral data and elemental analysis data of (OH)PcM: **11a-d**, (OFba)PcM: **12a-d**, and (OFbaC_{60})PcM: **3a-d**.

Compound	Mol. formula (Mol. wt)	Mass observed	Elemental analysis: Found(Calcd.)(%)			Yield (%)
			N	C	H	
11a : (OH)PcCo	$C_{224}H_{352}N_8O_{20}Co$ (3536.23)	3538.11	3.10(3.17)	76.4(76.08)	10.26(10.03)	20.5
11b : (OH)PcNi	$C_{224}H_{352}N_8O_{20}Ni$ (3535.99)	3537.22	3.17(3.17)	75.94(76.09)	10.15(10.03)	23.7
11c : (OH)PcCu	$C_{224}H_{352}N_8O_{20}Cu$ (3540.85)	3540.54	3.20(3.16)	76.14(75.98)	10.21(10.02)	29.5
11d : (OH)PcH_2	$C_{224}H_{354}N_8O_{20}$ (3479.32)	3482.63	3.13(3.22)	76.96(77.33)	10.61(10.26)	27.9
12a : (OFba)PcCo	$C_{232}H_{355}N_8O_{22}Co$ (3667.34)	3671.58	2.96(3.06)	76.15(75.98)	10.11(9.76)	87.3
12b : (OFba)PcNi	$C_{232}H_{355}N_8O_{22}Ni$ (3667.10)	3670.47	3.09(3.06)	75.72(75.99)	10.09(9.76)	98.7
12c : (OFba)PcCu	$C_{232}H_{355}N_8O_{22}Cu$ (3671.96)	3676.71	3.01(3.05)	76.24(75.89)	10.14(9.74)	65.0
12d : (OFba)PcH_2	$C_{232}H_{357}N_8O_{22}$ (3610.43)	3614.27	3.09(3.10)	77.23(77.18)	10.31(9.97)	66.5
3a: (OFbaC_{60})PcCo	$C_{294}H_{360}N_9O_{21}Co$ (4415.07)	4416.57, 3695.94	-	-	-	79.8
3b: (OFbaC_{60})PcNi	$C_{294}H_{360}N_9O_{21}Ni$ (4414.83)	4424.47, 3700.34	-	-	-	96.8
3c: (OFbaC_{60})PcCu	$C_{294}H_{360}N_9O_{21}Cu$ (4419.69)	4424.18, 3705.23	-	-	-	85.1
3d: (OFbaC_{60})PcH_2	$C_{294}H_{362}N_9O_{21}$ (4358.16)	4366.84, 3643.64	-	-	-	75.8

Table 2 Electronic spectral data of (OH)PcM: **11** (**a**=Co, **b**=Ni, **c**=Cu, and **d**=H_2), (OFba)PcM: **12** (**a**=Co, **b**=Ni, **c**=Cu, and **d**=H_2),and (OFbaC_{60})PcM:**3** (**a**=Co, **b**=Ni, **c**=Cu, and **d**=H_2).

Compound	Concentration[a] ($X10^{-5}$mol/l)	λmax (nm) (logε)			
		C_{60} peak	Soret-band	Q-band	
(OH)PcCo: **11a**	1.2		327.7 (4.9)	608.8 (4.6) 643.4 (sh)	677.1 (5.2)
(OH)PcNi: **11b**	1.0		289.4 (5.0) 306.6 (5.0) 330.3 (sh)	628.4 (4.6) 646.2 (sh)	675.6 (5.3)
(OH)PcCu: **11c**	1.8		290.8 (4.9) 340.2 (5.0)	615.4 (4.7) 651.8 (4.6)	686.7 (5.3)
(OH)PcH_2: **11d**	0.98		291.1 (4.8) 342.9 (4.9)	608.3 (4.4) 644.8 (4.6) 669.8 (5.1)	704.3 (5.1)
(OFba)PcCo: **12a**	1.0		327.1 (5.3)	608.6 (4.6) 642.7 (sh)	675.9 (5.2)
(OFba)PcNi: **12b**	1.0		288.6 (5.0) 305.3 (5.0) 330.2 (sh)	608.6 (4.6) 647.6 (sh)	675.9 (5.3)
(OFba)PcCu: **12c**	1.6		291.3 (4.9) 341.3 (4.9)	615.0 (4.6) 652.5 (sh)	685.0 (5.3)
(OFba)PcH_2: **12d**	1.2		291.5 (4.8) 345.3 (4.9)	607.4 (4.9) 643.9 (0.51) 670.0 (5.1)	702.8 (5.1)
(OFbaC_{60})PcCo: **3a**	0.63	245.0 (5.2)	292.8 (5.1)	609.2 (4.5) 642.9 (sh)	677.2 (5.2)
(OFbaC_{60})PcNi: **3b**	0.54	248.0 (5.1)	283.3 (5.0) 309.2 (5.0) 328.2 (sh)	610.9 (4.5) 647.8 (sh)	676.1 (5.1)
(OFbaC_{60})PcCu: **3c**	0.52	255.6 (5.2)	292.7 (sh) 340.3 (5.0)	618.1 (4.7) 652.2 (sh)	684.9 (5.2)
(OFbaC_{60})PcH_2: **3d**	0.53	254.5 (5.1)	288.6 (5.0) 338.8 (4.9)	610.9 (4.5) 641.4 (4.6) 669.7 (5.0)	704.3 (5.1)

a : in chloroform

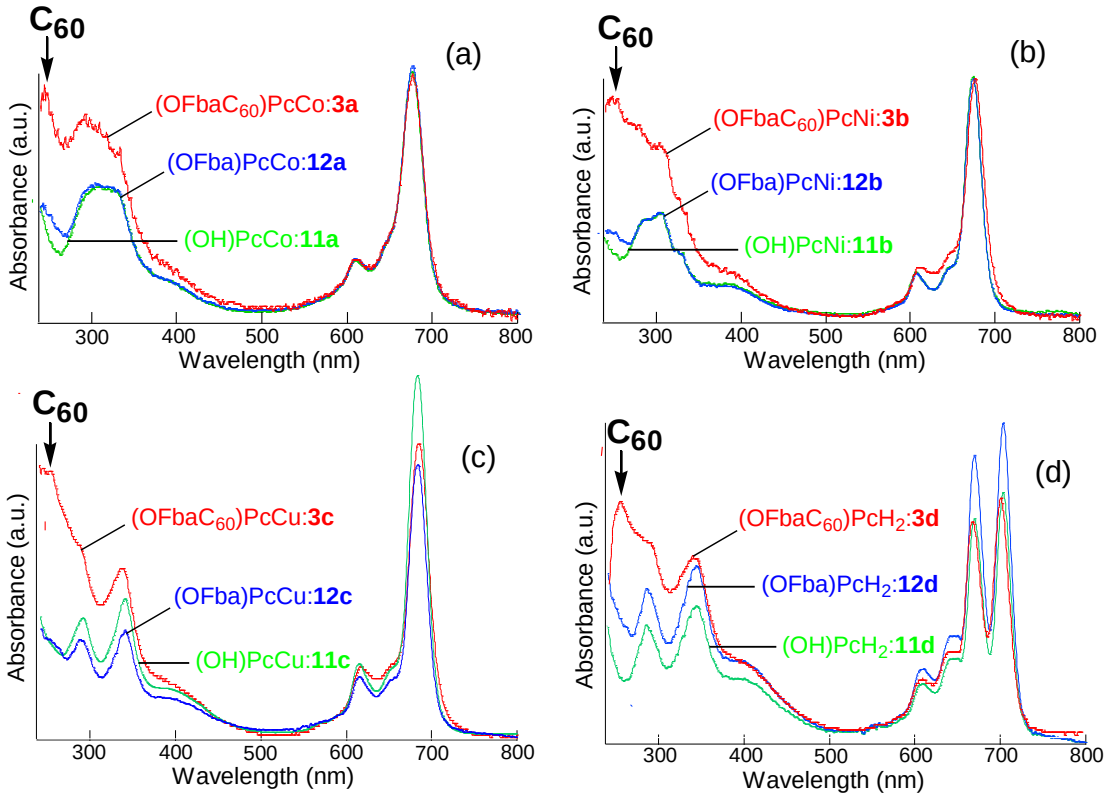

Fig. 2 UV-vis spectra in CH_3Cl at room temperature: (a) PcCo (**11a**, **12a**, and **3a**), (b) PcNi (**11b**, **12b**, and **3b**), (c) PcCu (**11c**, **12c**, and **3c**), (d) PcH_2 (**11d**, **12d**, and **3d**).

Table 3 Phase transition temperatures and enthalpy changes of all the compounds.

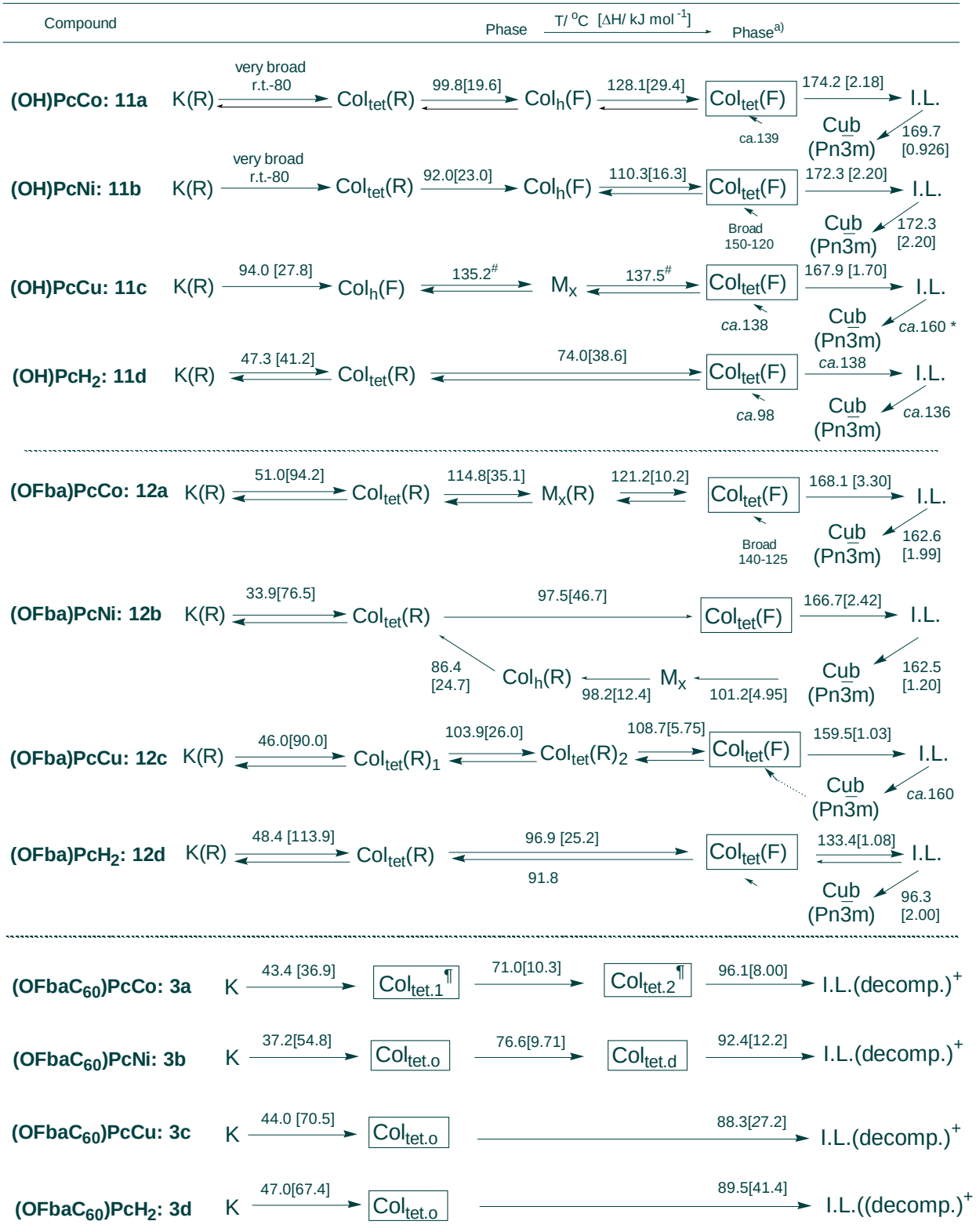

a) Phase nomenclature: K=crystal, Col_h=hexagonal columnar mesophase, $Col_{tet.o}$=tetragonal ordered columnar mesophase, $Col_{tet.d}$=tetragonal disordered columnar mesophase, M_x=unidentified mesophase, Cub=cubic mesophase, I.L.=isotropic liquid, (R) = roof-top-shaped dimer stacking and (F) = face-to-face stacking. * = the DSC peak was too small to estimate the enthalpy change, + = gradual decomposition after clearing, # = two peaks were too close to determine the enthalpy changes, ▭ = mesophase shawing homeotropic alignment, and ¶ = This mesophase gave only one XRD peak in the low angle region. Although the mesophase was impossible to be established from the one peak, it was tentatively identified as a Col_{tet} mesophase.

Table 4 X-ray data of (OH)PcM (**11a-d**), (OFba)PcM (**12a-d**) and (OFbaC_{60})PcM (**3a-d**).

Compound	Lattice constants/ Å	Spacing/ Å		Miller indices
		Observed	Calculated	(*h k l*)
(OH)PcCo: **11a**	Col_{tet}(R) at 85°C	33.2	33.2	(1 0 0)
	a = 33.2	23.0	23.5	(1 1 0)
	h_2 = *ca.*9.3	14.6	14.8	(2 1 0)
	h_1 = 4.89	*ca.*9.3	-	h_2
	Z= 0.92 for ρ = 1.0	4.89	-	h_1
		*ca.*4.5	-	#
	Col_h(F) at 115°C	33.7	33.7	(1 0 0)
	a = 38.9	19.9	19.5	(1 1 0)
		13.1	12.7	(2 1 0)
		*ca.*4.6	-	#
	Col_{tet}(F) at 160°C	30.2	30.5	(1 0 0)
	a = 30.5	21.5	21.5	(1 1 0)
		*ca.*4.6	-	#
	Cub(Pn3m) at 163°C on cooling	39.4	39.4	(3 2 1)
	a = 147	35.0	35.0	(3 3 0)
		33.4	33.4	(3 3 1)
		30.2	30.2	(4 2 2)
		20.5	20.5	(6 4 0)
		ca.13.2	-	#
		ca.9.4	-	#
		*ca.*4.7	-	#
		ca.3.6	-	h
(OH)PcNi: **11b**	Col_{tet}(R) at 80°C	33.7	33.7	(1 0 0)
	a = 33.7	23.0	23.8	(1 1 0)
	h_2 = *ca.*9.4	*ca.*9.4	-	h_2
	h_1 = 4.87	4.87	-	h_1
	Z = 1 for ρ = 1.2	*ca.*4.4	-	#
	Col_h(F) at 105°C	34.0	34.0	(1 0 0)
	a = 39.3	20.3	19.6	(1 1 0)
	h = *ca.* 3.5	13.3	12.9	(2 1 0)
	Z = 1 for ρ = 1.2	ca. 9.0	-	#
		*ca.*4.5	-	#
		*ca.*3.5	-	h
	Col_{tet}(F) at 130°C	31.5	31.2	(1 0 0)
	a = 31.2	22.1	22.1	(1 1 0)
		*ca.*4.6	-	#
	Cub(Pn3m) at 160°C on cooling	34.5	34.5	(3 2 1)
	a = 129	30.7	30.7	(3 3 0)
		29.6	29.6	(3 3 1)
		21.9	21.9	(5 3 1)
		ca.8.9	-	#
		ca.4.6	-	#
		ca.3.4	-	h
(OH)PcCu: **11c**	Col_h(F) at 120°C	34.5	34.5	(1 0 0)
	a = 40.7	20.3	19.9	(1 1 0)
		17.3	17.2	(2 0 0)
		13.1	13.0	(2 1 0)
		11.6	11.5	(3 0 0)
		*ca.*4.4	-	#
	Col_{tet}(F) at 160°C	30.7	30.9	(1 0 0)
	a = 30.9	21.9	21.9	(1 1 0)
		*ca.*9.6	-	#
		*ca.*4.7	-	#
	Cub(Pn3m) at 154°C on cooling	38.4	38.4	(3 2 1)
	a = 144	34.0	34.0	(3 3 0)
		33.2	33.2	(3 3 1)
		32.0	32.0	(4 2 0)
		30.9	30.9	(3 3 2)
		22.6	22.7	(6 2 1)
		ca.8.6	-	#
		ca.4.6	-	#
		ca.3.5	-	h

= Halo of the molten alkoxy chains. h_1 = stacking distance between the monomers. h_2 = stacking distance between the dimers. ¶ = This mesophase gave only one XRD peak in the low angle region. Although the mesophase was impossible to be established from the one peak, it was tentatively identified as a Coltet mesophase.

Table 4 (Continued)

(OH)PcH$_2$: **11d**	M_x(R) at 70^{o}C If this mesophase is Col$_{tet}$(R), a = 35.9.	35.9 22.4 *ca.*9.5 4.81 *ca.*4.5	- - - - -	- - h_2 h_1 #
	Col$_{tet}$(F) at 110^{o}C a = 34.5	34.5 24.4 *ca.*4.5	34.5 24.4 -	(1 0 0) (1 1 0) #
	Cub(Pn3m) at 130^{o}C on cooling a = 129	38.7 37.1 32.5 23.7 *ca.*4.5	39.0 37.3 32.3 23.6 -	(3 1 1) (2 2 2) (4 0 0) (5 2 1) #
(OFba)PcCo: **12a**	Col$_{tet}$(R)$_1$ at 85^{o}C a = 32.5 h_2 = ca.9.5 h_1 = 4.89 Z = 0.88 for ρ = 1.0	33.2 23.0 14.6 *ca.*9.5 4.89 *ca.*4.5	32.5 23.0 14.5 - - -	(1 0 0) (1 1 0) (2 1 0) h_2 h_1 #
	M_x at 118^{o}C If this mesophase is Col$_{tet}$(R)$_2$, a=32.2.	32.2 21.2 13.3 ca.9.5 4.89 ca.4.5	- - - - - -	- - - h_2 h_1 #
	Col$_{tet}$(F) at 160^{o}C a = 30.6	30.2 21.6 11.0 *ca.*4.6	30.6 21.6 10.8 -	(1 0 0) (1 1 0) (2 2 0) #
	Cub(Pn3m) at 155^{o}C on cooling a = 140	37.4 32.9 32.0 29.8 22.2 *ca.*9.9 *ca.*4.7 *ca.*3.4	37.4 32.9 32.0 29.8 22.2 - - -	(3 2 1) (3 3 0) (3 3 1) (3 3 2) (6 2 0) # # h
(OFba)PcNi: **12b**	Col$_{tet}$(R) at 90^{o}C a = 33.2 h_2 = *ca.*9.3 h_1 = 4.85 Z = 0.83 for ρ = 1.0	32.2 21.7 13.5 11.0 *ca.*9.3 4.85 *ca.*4.5	32.2 22.8 14.4 10.7 - - -	(1 0 0) (1 1 0) (2 1 0) (3 0 0) h_2 h_1 #
	Col$_{tet}$(F) at 160^{o}C a = 30.5	30.0 21.5 ca.9.0 *ca.*4.7 *ca.*3.5	30.5 21.5 - - -	(1 0 0) (1 1 0) # # h
	Cub(Pn3m) at 155^{o}C on cooling a = 124	39.1 37.7 35.6 32.7 29.6 21.9 *ca.*9.2 *ca.*4.6 *ca.*3.5	39.0 37.7 35.6 32.7 29.6 21.8 - - -	(3 1 0) (3 1 1) (2 2 2) (3 2 1) (3 3 0) (4 4 0) # # h
	Col$_h$(R) at 90^{o}C on cooling a = 41.3 h_2 = *ca.*9.5 h_1 = 4.85 Z = 1.2 for ρ = 1.0	35.0 20.6 17.9 13.7 *ca.*9.5 4.85 *ca.*4.4	35.0 20.6 17.9 13.5 - - -	(1 0 0) (1 1 0) (2 0 0) (2 1 0) h_2 h_1 #

Table 4 (Continued)

(OFb a)PcCu: **12c**	$Col_{tet}(R)_1$ at 80°C a = 32.3 h = 4.85	32.7 22.9 *ca.*12 4.85 *ca.*4.3	32.3 22.9 - - -	(1 0 0) (1 1 0) (2 2 0)+(3 0 0) h #
	$Col_{tet}(R)_2$ at 107°C a = 35.0	35.0 23.2 17.7 *ca.*12 8.73 *ca.*4.4	35.0 24.8 17.5 *ca.*12 8.76 -	(1 0 0) (1 1 0) (2 0 0) (2 2 0)+(3 0 0) (4 0 0) #
	$Col_{tet}(F)$ at 145°C a = 31.1	31.1 22.5 *ca.*12 *ca.*4.3	31.1 22.0 - -	(1 0 0) (1 1 0) (2 2 0)+(3 0 0) #
	Cub(Pn3m) at 155°C a = 128	38.7 37.1 34.0 30.7 ca.12.2 *ca.*4.4	38.7 37.0 33.9 30.6 - -	(3 1 1) (2 2 2) (3 2 1) (3 3 0) # #
(OFb a)PcH_2: **12d**	$Col_{tet}(R)$ at 80°C a = 33.4 h = 4.84	33.4 23.5 14.4 11.1 4.84 *ca.*4.4	33.4 23.5 15.0 11.1 - -	(1 0 0) (1 1 0) (2 1 0) (3 0 0) h #
	$Col_{tet}(F)$ at 110°C a = 32.0	32.0 22.9 14.0 *ca.*4.4	32.0 22.6 14.3	(1 0 0) (1 1 0) (2 1 0) #
	Cub(Pn3m) at 125°C a = 138	39.4 34.8 31.5 30.7 21.9 ca.12.8 *ca.*4.4	39.3 34.7 31.5 30.6 21.8 - -	(2 2 2) (4 0 0) (3 3 1) (4 2 0) (6 2 0) # #
(OFb aC_{60})PcCo: **3a**	$Col_{tet.1}$¶ at 65°C a = 33.2	33.2 *ca.*9.8 *ca.*4.5	33.2 - -	(1 0 0) # #
	$Col_{tet.2}$¶ at 90°C a = 33.7	33.7 *ca.*9.5 *ca.*4.7	33.7 - -	(1 0 0) # #
(OFb aC_{60})PcNi: **3b**	$Col_{tet.o}$ at 70°C a = 33.4 h = 4.84	33.4 14.2 *ca.*9.3 4.84 *ca.*4.4	33.4 15.0 - - -	(1 0 0) (2 1 0) # h #
	$Col_{tet.d}$ at 90°C a = 33.2	33.2 23.6 *ca.*9.2 *ca.*4.5	33.2 23.5 - -	(1 0 0) (1 1 0) # #
(OFb aC_{60})PcCu: **3c**	$Col_{tet.o}$ at 90°C a = 33.2 h = 4.85	33.2 23.4 ca.11.5 4.85 *ca.*4.5	33.2 23.5 - - -	(1 0 0) (1 1 0) # h #
(OFb aC_{60})PcH_2: **3d**	$Col_{tet.o}$ at 75°C a = 34.0 h = 4.81	34.0 23.9 *ca.*9.1 4.81 *ca.*4.5	34.0 24.0 - - -	(1 0 0) (1 1 0) # h #

(a) Parallel(cofacial) transition dipoles: Blue-shift case

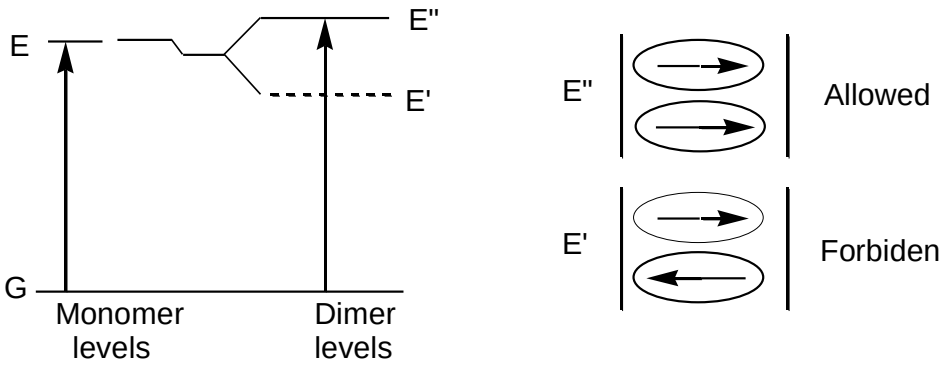

(b) In-line transition dipoles: Red-shift case

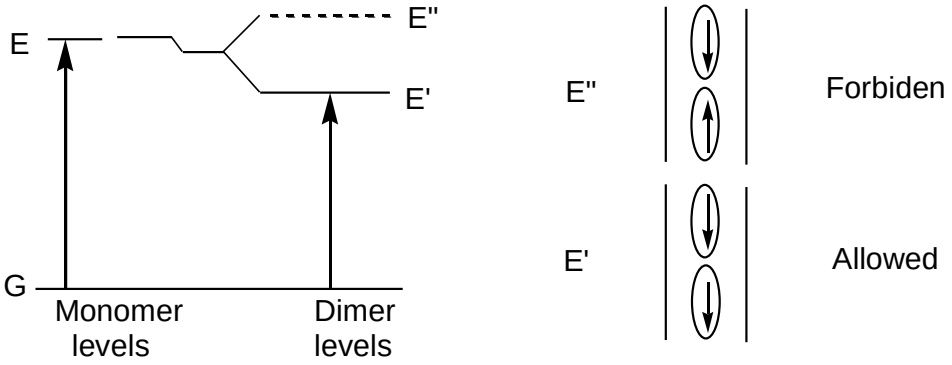

(c) Co-planar(slipped) transition dipoles: Shift depends on angle θ.

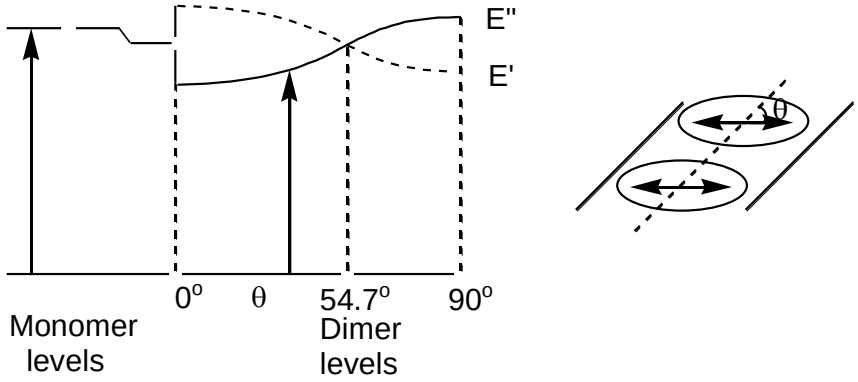

(d) Oblique(herringbone) transition dipoles: Band-splitting case

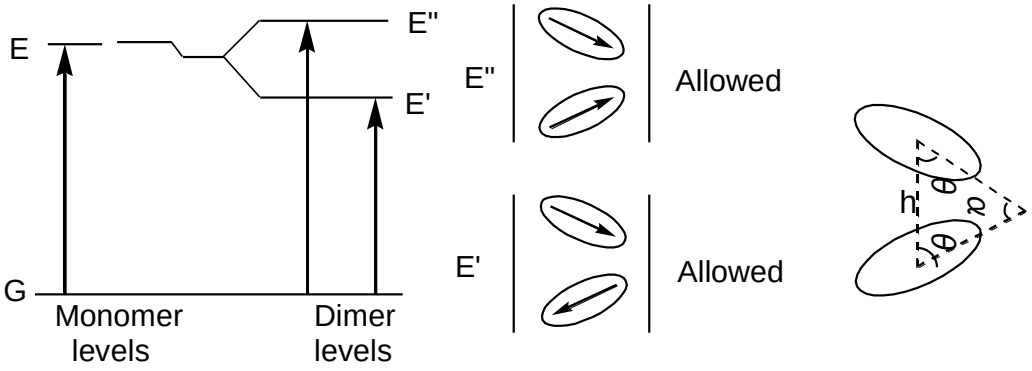

Fig. 3 Kasha's rules: exciton energy diagrams for various dimers.

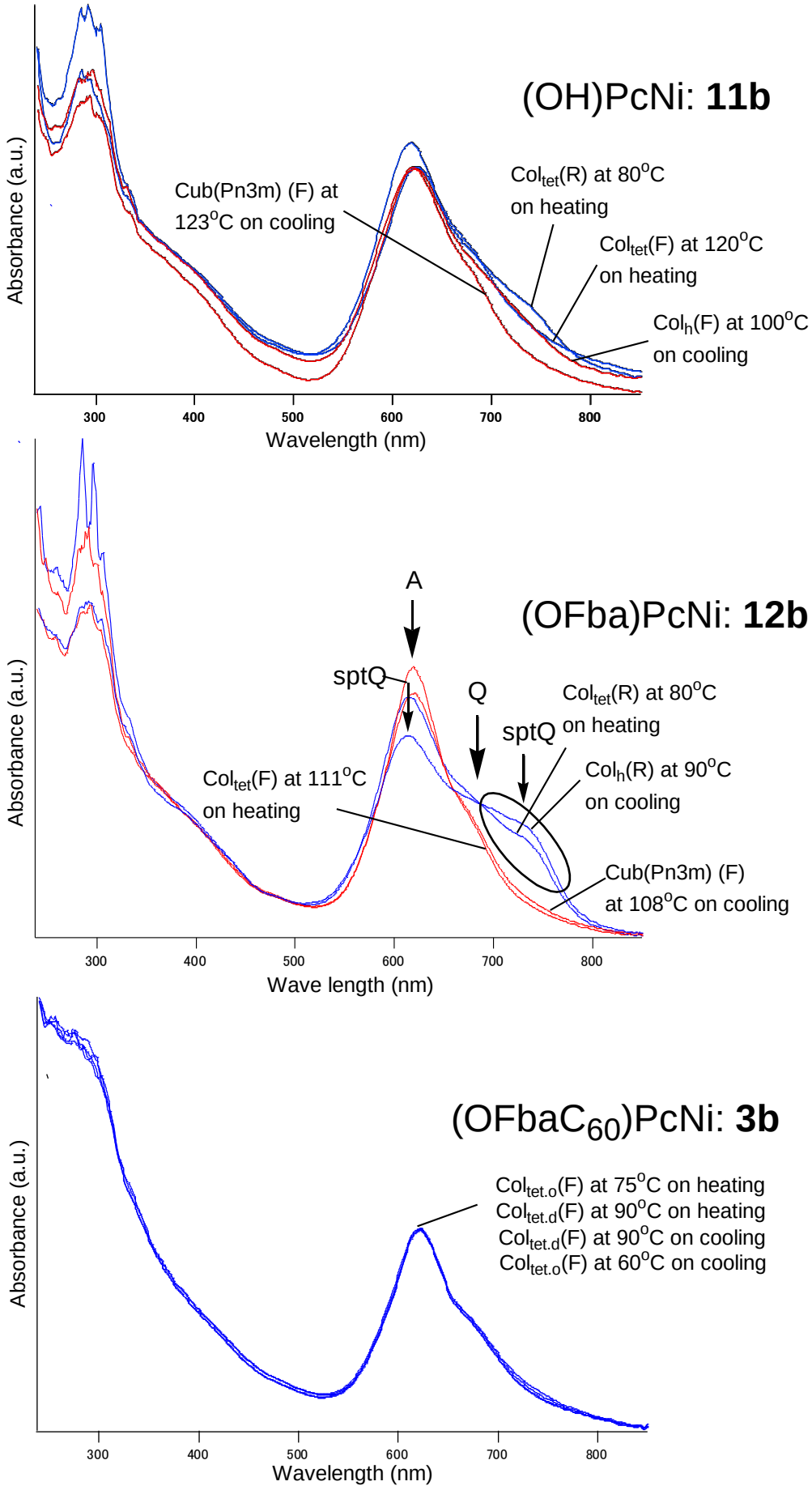

Fig. 4 UV-vis spectra of the thin films of (OH)PcNi: **11b**, (OFba)PcNi: **12b**, and (OFbaC$_{60}$)PcNi: 3b. Q = Q band; SptQ = split Q bqand**;** A = aggregated band**.**

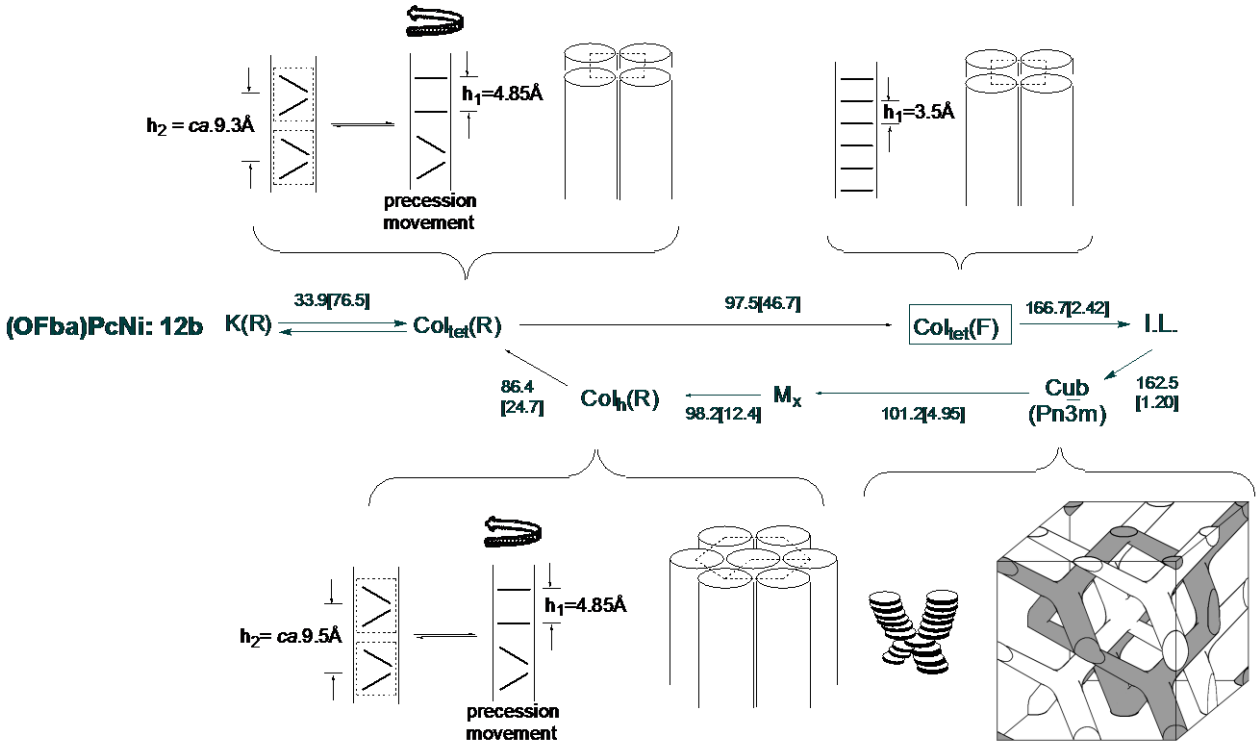

Fig. 5. The mechanism of phase transition for (OFba)PcNi (12b).

Table 5 Phase transition temperatures and enthalpy changes of the previous PuCu(OCH_3) compounds (**8**, **9** and **2**) and the present Cu compounds (**11c, 12c** and **3c**).

Compound	Phase T/ °C [ΔH/ kJ mol $^{-1}$] Phase[a)]
(OH)PcCu(OCH_3): 8	K 30-70 [101] Col_{h1} 142.3 [16.5] Col_{h2} 153.1 Col_{h3} 154.1 Col_{tet} very slow Cub (Pn3m) 182.6 I.L. 180.8; [3.10]; 182.0 [2.33] I.L.; 153.3 [4.89]
(OH)PcCu: 11c	K(R) 94.0 [27.8] $Col_h(F)$ 135.2# M_x 137.5# $Col_{tet}(F)$ 167.9 [1.70] I.L.; *ca.*138; Cub (Pn3m) *ca.*160 *
(OFba)PcCu(OCH_3): 9	K 40.6 [73.8] Col_{ob1} 73.8 [10.8] Col_{ob2} 116.5 Col_{ob3} *ca.* 122 Col_{tet} 170.8 [1.9] I.L.; [17.8]
(OFba)PcCu: 12c	K(R) 46.0[90.0] $Col_{tet}(R)_1$ 103.9[26.0] $Col_{tet}(R)_2$ 108.7[5.75] $Col_{tet}(F)$ 159.5[1.03] I.L.; Cub (Pn3m) *ca.*160
($OFbaC_{60}$)PcCu(OCH_3): 2	Col_{tet1} 44.9 [69.5] Col_{tet2} 88.6 [20.4] Col_{tet3} 167.2 [10.0] I.L.
($OFbaC_{60}$)PcCu: 3c	K 44.0 [70.5] $Col_{tet.o}$ 88.3[27.2] I.L.(decomp.)$^+$

a) Phase nomenclature: K = crystal, Col_h = hexagonal columnar mesophase, $Col_{tet.o}$ = tetragonal ordered columnar mesophase, $Col_{tet.d}$ = tetragonal disordered columnar mesophase, M_x = unidentified mesophase, Cub = cubic mesophase, I.L. = isotropic liquid, + = gradual decomposition over *ca.*120°C, and ☐ = mesophase shawing homeotropic alignment.

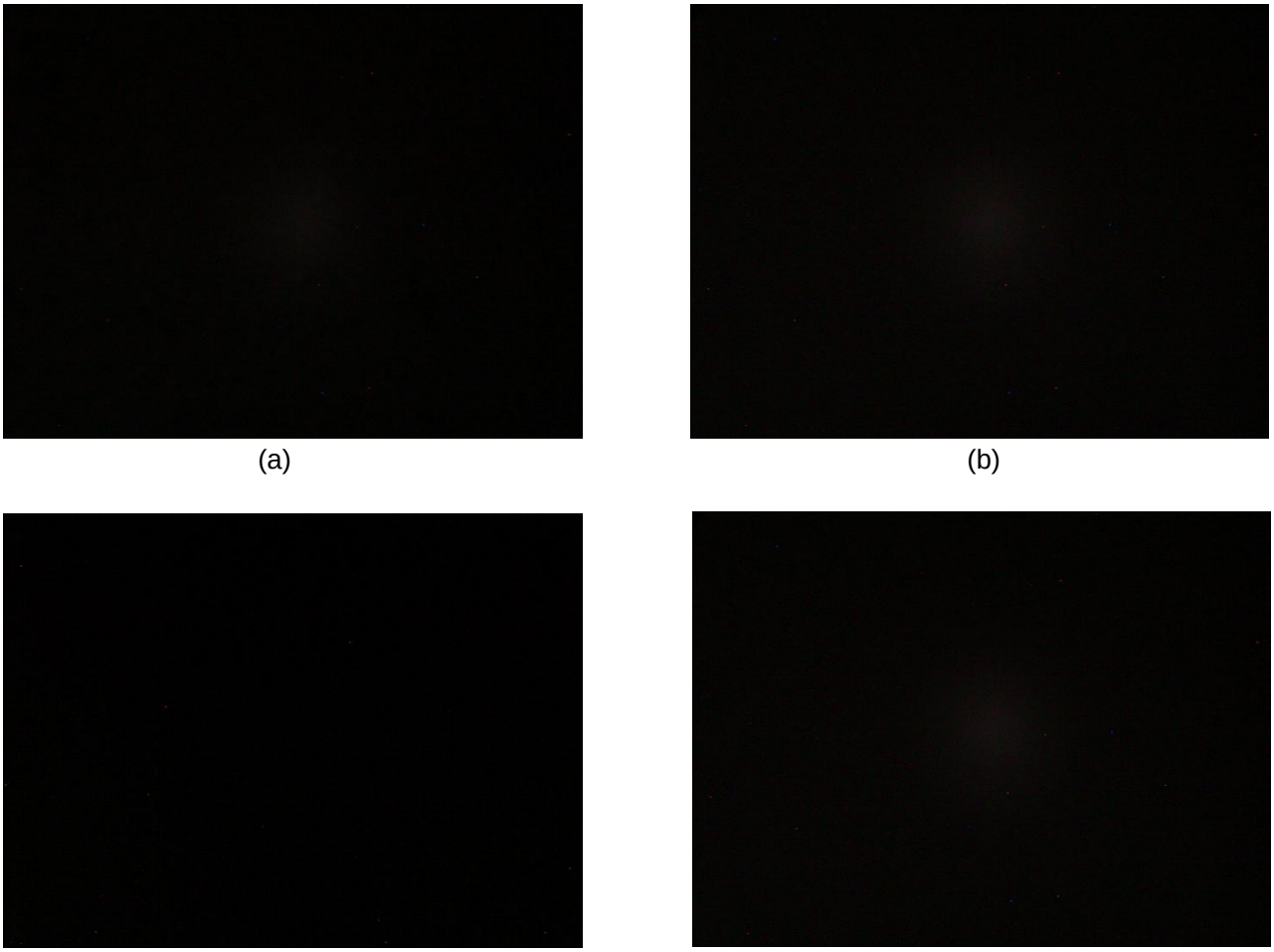

Fig. 6 Photomicrographs of the (OFbaC$_{60}$)PcM: (a) (OFbaC$_{60}$)PcCo: **3a** at 90.0^{o}C on the 1st heating, (b) (OFbaC$_{60}$)PcNi: **3b** at 85.0 ^{o}C on the 1st heating, (c) (OFbaC$_{60}$)PcCu: **3c** at 87.0^{o}C on the 1st heating, and (d) (OFbaC$_{60}$)PcH$_2$: **3d** at 87.0^{o}C on the 1st heating (all the photos were taken under crossed polarizers.)